HHS Public Access

Author manuscript

Biomed Microdevices. Author manuscript; available in PMC 2016 May 04.

Published in final edited form as:

Biomed Microdevices. 2016 April ; 18(2): 30. doi:10.1007/s10544-016-0057-z.

Polyethersulfone improves isothermal nucleic acid amplification compared to current paper-based diagnostics

J. C. Linnes[1,2], **N. M. Rodriguez**[1], **L. Liu**[1], and **C. M. Klapperich**[1]

C. M. Klapperich: catherin@bu.edu

[1]Department of Biomedical Engineering, Boston University, Boston, MA 02215, USA

[2]Weldon School of Biomedical Engineering, Purdue University, West Lafayette, IN 47907, USA

Abstract

Devices based on rapid, paper-based, isothermal nucleic acid amplification techniques have recently emerged with the potential to fill a growing need for highly sensitive point-of-care diagnostics throughout the world. As this field develops, such devices will require optimized materials that promote amplification and sample preparation. Herein, we systematically investigated isothermal nucleic acid amplification in materials currently used in rapid diagnostics (cellulose paper, glass fiber, and nitrocellulose) and two additional porous membranes with upstream sample preparation capabilities (polyethersulfone and polycarbonate). We compared amplification efficiency from four separate DNA and RNA targets (*Bordetella pertussis, Chlamydia trachomatis, Neisseria gonorrhoeae*, and Influenza A H1N1) within these materials using two different isothermal amplification schemes, helicase dependent amplification (tHDA) and loop-mediated isothermal amplification (LAMP), and traditional PCR. We found that the current paper-based diagnostic membranes inhibited nucleic acid amplification when compared to membrane-free controls; however, polyethersulfone allowed for efficient amplification in both LAMP and tHDA reactions. Further, observing the performance of traditional PCR amplification within these membranes was not predicative of their effects on *in situ* LAMP and tHDA. Polyethersulfone is a new material for paper-based nucleic acid amplification, yet provides an optimal support for rapid molecular diagnostics for point-of-care applications.

Keywords

Paper-based diagnostic device; Point-of-care diagnostics; Isothermal nucleic acid amplification; Polyethersulfone

1 Introduction

As paper-based devices for point-of-care diagnostics have been developed, a few membranes have dominated the literature due to their controlled flow, analyte separation, and reagent binding and release properties. Common examples include cellulose chromatography paper

Correspondence to: C. M. Klapperich, catherin@bu.edu.

Electronic supplementary material The online version of this article (doi:10.1007/s10544-016-0057-z) contains supplementary material, which is available to authorized users.

for separation and wicking, glass fiber for reagent release, and nitrocellulose for hybridization and protein binding. These paper materials are excellent for colorimetric chemical detection (e.g. urinalysis dipsticks) and protein-based immunoassays (e.g. rapid diagnostic tests for pregnancy and malaria), and it is tempting to choose these materials for use in the emerging field of paper-based nucleic acid amplification as well. Indeed, a number of researchers have selected from these materials to investigate such paper-based rapid molecular devices for point-of-care diagnostics (Ali et al. 2009; Liu et al. 2011; Rohrman and Richards-Kortum 2012; Gan et al. 2014; Linnes et al. 2014; Cordray and Richards-Kortum2015). These devices are easily disposable, have integrated fluidic pumping via capillary action, and act as solid supports for *in situ* molecular amplification. However, material selection, which is integral to efficient *in situ* nucleic acid amplification, has not yet been systematically explored in the majority of nucleic acid amplification strategies.

PCR is the predecessor to isothermal amplification strategies and has been used for many years in the analysis of dried-blood spots to detect HIV infections in remote settings by mailing cellulose paper membranes spotted with blood samples to central laboratories for nucleic acid amplification (Li et al. 2004). These samples traditionally require elution from the capture membranes because of the blood and material incompatibility with PCR. However, rapid molecular diagnostics that amplify nucleic acids directly from membranes *in situ* would provide the ability to detect pathogens on-site, even when far from core laboratory facilities. Many isothermal amplification strategies, including loop-mediated isothermal amplification (LAMP) and thermophilic helicase dependent amplification (tHDA), have recently been employed in these types of integrated sample-to-answer rapid molecular diagnostic devices using paper membranes (Connelly et al. 2015; Rodriguez et al. 2016). The ability to perform nucleic acid amplification without the precise thermal cycling required of PCR improves both the time-to-result and minimizes the power requirements of these reaction schemes for use at the point of care (Li and Macdonald 2015). Optimal paper-based rapid molecular diagnostic device design provides low-cost, highly efficient amplification across a range of nucleic acid targets and isothermal reaction schemes.

In our recent work with paper-based isothermal amplification of *Chlamydia trachomatis* (*C. trachomatis*) DNA, we observed that isothermal amplification efficiency was significantly improved when the tHDA mastermix was not fully absorbed into the paper support. Instead, when reagents were in contact with the captured nucleic acid targets on the support but excess liquid remained, amplification efficiency was greatly increased (unpublished observations). Despite the porous nature of the cellulose support, amplification was inhibited when all reagents were absorbed into the membrane without excess liquid. A previous publication by Rohrman et al. found that recombinase polymerase amplification (RPA) was also slightly inhibited when performed within cellulose matrix as compared to amplification in bound glass fibers (Rohrman and Richards-Kortum 2012). However, in detecting the H1N1 strain of Influenza A, we found no such inhibition of LAMP using porous polyethersulfone membranes (Rodriguez et al. 2015).We began to question whether current paper-based diagnostic membranes were actually the most appropriate materials for *in situ* isothermal amplification in these point-of-care devices.

The optimal design of amplification membranes is integral to performing paper-based isothermal molecular diagnostics at the point of care. Yet, membrane dependent amplification efficiency is still unknown for the majority of these techniques. Instead, most researchers have used easily available paper diagnostic materials with little regard to the effects that these material choices have on the performance of their nucleic acid amplification devices. Here, we sought to rectify this by systematically investigating the use of five separate membranes on the amplification efficacies of LAMP, tHDA, and PCR for a variety of pathogen nucleic acids. To encompass the most expansive uses for these membranes, we considered their effects both on amplification reactions performed in the presence of the membranes with excess liquid available, as well as on reactions in which the entirety of the liquid was absorbed into the porous matrices. We compared the traditional cellulose, glass fiber, and nitrocellulose diagnostic membranes with polyethersulfone (PES) and polycarbonate (PC) membranes that are commonly used as filtration media and would be of use when integrating amplification with upstream sample preparation steps.

2 Methods

2.1 Material samples

Paper membranes were chosen for analysis based on their use in either cell filtration, nucleic acid capture, or current point-of-care diagnostics. Paper samples used in this study were 0.34 mm thick 3MM Chr cellulose (CHR), 0.22 μm nominal pore size polyethersulfone (PES), 0.2 μm pore size track etched polycarbonate (PC), binder-free glass microfiber (GF) for 0.7 μm particle filtration, and 0.45 μm pore size nitrocellulose (NC). CHR, GF, and NC were purchased from GE Healthcare (Pittsburgh, PA), catalog numbers 3MM CHR (3030861), GF/F (1825–090), and Protran BA85 (10402506), respectively. PES and PC were purchased from Millipore EMD (Billerica, MA), catalog numbers GPWP04700 and GTTP14250, respectively.

2.2 Material characterization

2.2.1 SEM—Scanning electron microscopy (SEM) was performed using a Zeiss Supra 55VP field emission SEM (Oberkochen, Germany) to visualize the surface morphologies of the materials. Each of the paper matrices were punched using a 2 mm biopsy punch and were gold coated in a Cressington 108 manual sputter coater (Watford, England) prior to imaging in order to prevent charging of the surface. Samples were imaged at both 1000× and 5000× magnification.

2.2.2 Porosity—Porosity, defined as the percentage of void volume of the materials, was analyzed in the 5000× magnification SEM images via image J (NIH, Bethesda, MA) using the Particle Analysis feature (Ferreiera and Rasband 2012). This porosity measurement assumes uniform size and distribution of pores and pore sizes throughout the thickness of each material. Briefly, the image threshold was set by eye to exclude only features on the front-most surfaces of the material while including pores and background features in the samples. The Particle Analysis was adjusted to include all pores with pixel area equal or greater than 2 pixels^2 (equivalent to 15.5 nm diameter at the 5000× magnification) and circularity from 0 to 1.0 as well as including all edge boundaries. Porosity was determined

as the area of the image that was included in the threshold divided by the total image area. The total number of pores per 100 μm^2, their size, and diameter were also included in the analysis although these measurements were excluded from the CHR and GF as these materials are made of matted fibers rather than pores.

2.2.3 Water absorbency—The water absorbency of each of the five different materials (CHR, PES, PC, GF, and NC) was measured by calculating the difference in weight before and after submerging a 1 cm by 1 cm square of the material in deionized water as described by Rohrman et al. (Rohrman and Richards-Kortum 2012). The materials were submerged until fully wetted and then gently blotted onto a polystyrene weight dish to remove excess liquid before weighing. Measurements were taken using a Metler Toledo (Columbus, OH) brand Analytical Balance with resolution down to 0.1 mg from five replicate samples for each paper. The average and standard deviation of the water absorbency were determined from the replicate samples. This average measurement was used to calculate the amount of liquid absorbed into the papers during amplification of DNA from 6 cm diameter coupons, as well as calculating the area of paper material needed to absorb a full 25 μL of liquid.

2.3 DNA/RNA

Quantified genomic DNA from *Bordetella pertussis* (*B. pertussis*) strain Tahoma I was purchased from American Type Cell Culture (ATCC, Manassas, VA). Quantified genomic DNA from *Chlamydia trachomatis* (*C. trachomatis*) strain 434 LGV II was purchased from Advanced Biotechnologies, Inc. (Eldersburg, MD). Frozen stocks of each DNA type were aliquotted to 1.5 ng/μl and stored at −20 °C until use.

Neisseria gonorrhoeae (*N. gonorrhoeae*) strain NCTC 8375 was kindly provided by BioHelix, Inc. (Beverly, MA). *N. gonorrhoeae* was cultured on BD Chocolate Agar (Heidleberg, Germany) at 37 °C with 5 % CO_2 for 48 h. Genomic DNA was then purified from *N. gonorrhoeae* plate cultures using a QIAamp DNA Mini Kit (QIAgen Inc., Valencia, CA) according to the manufacturer's instructions with the following modification: DNA was eluted into nuclease-free water instead of the provided EB buffer. The concentration of the purified DNA was determined by measuring the OD_{260} with a NanoDrop ND-2000c (Thermo Scientific, Waltham, MA). The quantity of DNA was calculated, and 100 μl aliquots of 1.8 ng/μl were made and stored at −20 °C.

Influenza A (H1N1) *in vitro* RNA standards containing both target regions of the HA gene for the RT-LAMP and RT-PCR assays were generated by cloning the viral genomic RNA from a de-identified patient sample that tested positive for H1N1. Briefly, RNA from the patient sample was extracted via a Qiagen Viral Mini Kit and reverse-transcribed with a Superscript III cDNA synthesis kit (Life Technologies, Grand Island, NY) with a gene-specific reverse primer. The target region of the HA gene from position HA_351 to HA_1735 was amplified by PCR with a Phusion High-Fidelity PCR kit (New England BioLabs, Ispwitch, MA), purified via a QIAgen gel extraction kit, and cloned into a pGEM-T Easy vector (Promega, Masidon, WI). Plasmids were purified with a QIAgen Midi Prep Kit, blunt-cut linearized, and served as *in vitro* transcription DNA templates using a ProMega Ribomax Transcription kit. The RNA transcripts were then purified via acid

phenol-chloroform extraction and ethanol precipitation. The concentration of the purified RNA was determined by measuring the OD_{260} with the NanoDrop ND-2000c apparatus (Thermo Scientific, Waltham, MA). The target RNA copy number was calculated, and 50 µl aliquots were made and stored at −70 °C.

2.4 Nucleic acid amplification

All amplification experiments were carried out in individual 0.2 ml reaction tubes containing CHR, PES, PC, GF, or NC. An additional positive control reaction containing DNA/RNA without paper and a negative control reaction containing master mix and nuclease-free water only were included in every experiment. For experiments testing amplification in the presence of a paper matrix, 6 mm diameter hole punches of each paper material were used. None of the 6 mm coupons held a full 25 µl of reaction liquid. Therefore, for experiments testing amplification completely within a paper matrix, materials were cut to the appropriate size needed to absorb the 25 µL reaction based on their measured water absorbency. The sizes used for amplification within paper without excess liquid were 0.6 cm^2, 0.6 cm^2, 1.8 cm^2, 0.3 cm^2, and 0.9 cm^2 for CHR, PES, PC, GF, and NC, respectively. Preliminary experiments were performed to adjust the primer ratios, salt, and amplification stabilization reagent concentrations as necessary to ensure the maximum amplification efficiency of each reaction in the liquid phase prior to testing amplification in the presence of the paper membranes.

Cut or hole-punched paper materials were placed into PCR strip-tubes. Five microliters of the RNA or DNA templates were pipetted directly onto each of the paper membranes. Twenty microliters of the appropriate amplification master mix were then added directly onto each of the paper surfaces. The tubes were incubated as described for each isothermal or PCR condition. Following amplification, a hole was made at the bottom of each tube using a sterile 18-gauge syringe needle. The tubes were stacked onto a clean 96-well plate and centrifuged at 2500 rpm for 1 min to elute any liquid absorbed by the papers and collect it into the plate wells for downstream detection by gel electrophoresis and lateral flow strip as described in the Detection section. All experiments were repeated three separate times for every reaction condition.

2.4.1 Nucleic acid amplification chemicals—Bst and Taq polymerases, associated reaction buffers, and magnesium sulfate were purchased from New England Biolabs (Ipswich, MA). Betaine was purchased from Sigma Aldrich (St. Louis, MO), dNTPs and Thermoscript Reverse Transcriptase from Life Technologies (Carlsbad, CA). Superscript III Platinum One-Step quantitative kit, EvaGreen from Biotium (Hayward, CA) and ROX reference dye were purchased from Invitrogen (Carlsbad, CA). All primers, labeled primers, and probes were purchased from Integrated DNA Technologies (Coralville, IA).

2.4.2 Loop-mediated isothermal amplification (LAMP)

***B. pertussis* LAMP:** *B. pertussis* genomic DNA was amplified using LAMP at 65 °C for 20 min. The reaction was carried out in a final volume of 25 µl with 5 µl of 150 pg/µl genomic DNA, 8 U large fragment Bst polymerase and 1× ThermoPol Reaction Buffer, 0.8 M Betaine, 2 mM $MgSO_4$, 1 mM each dNTP, 7.5 pmol each of forward and reverse outer

primers, 30 pmol each of forward and reverse loop primers, 75 pmol each of forward and reverse inner primers, and EvaGreen and ROX reference dyes for real-time quantitative analysis of positive and negative controls. Forward and reverse loop primers were tagged with 6-carboxyfluorescein (FAM) and biotin, respectively, to enable immediate downstream detection of the amplified products on lateral flow detection (LFD) strips. Primer sequences were previously developed by Kamachi et al. and are described in Table S1 (Kamachi et al. 2006).

Influenza A (H1N1) RT-LAMP: Influenza A (H1N1) virus RNA was amplified via reverse-transcription LAMP (RT-LAMP) at 65 °C for 15 min. The reaction was carried out in a final volume of 25 μl with 5 μl of 10^6 copies/μL cloned H1N1 RNA, 8 U large fragment Bst 2.0 DNA polymerase and 1× Isothermal Amplification Buffer, 2 U Thermoscript Reverse Transcriptase, 0.8 M Betaine, 8 mM $MgSO_4$, 1 mM each dNTP, 5 pmol each of forward and reverse outer primers, 20 pmol each of forward and reverse loop primers, 40 pmol each of forward and reverse inner primers, and SybrGreen and ROX reference dyes for real-time quantitative analysis of positive and negative controls. As with *B. pertussis*, forward and reverse loop primers were tagged with FAM and biotin, respectively, to enable downstream detection of the amplified products on LFD strips. Primer sequences previously described by Kubo et al. 2010 were used and are available in Table S1 (Kubo et al. 2010).

2.4.3 HDA

***N. gonorrhoeae* tHDA:** tHDA of *N. gonorrhoeae* genomic DNA was performed according to the manufacturer's instructions (Quidel, San Diego, CA). A 20 μl master mix for tHDA was made using final concentrations of 90 nM forward primer tagged with a 3′ biotin, 30 nM reverse primer, and 30 nM FAM labeled probe, with 10 % ficoll 400, 1 U MboI restriction enzyme. Primer and probe sequences are described in Table S1. Mastermix was added to 5 μl of *N. gonorrheae* DNA at a concentration of 180 pg/μl and overlaid with 50 μl of mineral oil. The reactions were amplified at 65 °C for 30 min. Biotin and FAM labelled amplicons were detected via LFD strips.

***C. trachomatis* tHDA:** tHDAof *C. trachomatis* genomic DNA was performed at 65 °C for 30 min according the manufacturer's instructions (Quidel, San Diego, CA). The 20 μl master mix included 10 % ficoll 400, 1 U Hpy188II restriction enzyme, 40 nM forward primer, 90 nM 3′-biotinylated reverse primer, 30 nM FAM labeled probe. Previously published primer and probe sequences are described in Table S1 (Linnes et al. 2014). Master mix was added to 5 μl of 150 pg/μl *C. trachomatis* DNA. The reagents were overlaid with 50 μl of mineral oil prior to amplification. Downstream detection in LFD utilized amplicons labeled with biotin and FAM.

2.4.4 PCR—Real-time PCR on *N. gonorrhoeae, C. trachomatis*, and *B. pertussis* were performed using Taq DNA polymerase according to the manufacturer's protocol. PCR primers targeting *C. trachomatis* cryptic plasmid ORF3 gene and *N. gonorrhoeae* porA pseudogene were designed using PrimerQuest (IDT, Coralville, IA). TaqMan PCR targeted *B. pertussis* insertion sequence IS481 as described by Reischl et al. (Reischl et al. 2001). Magnesium chloride concentrations were optimized to 3 mM final reaction concentrations

for *C. trachomatis* and *N. gonorrhoeae* PCR reactions and 1mMfor *B. pertussis* amplification. Five microliters of appropriate DNA at 150 pg/μL were used as the template in each reaction and pipetted directly onto the paper substrates. Twenty microliters of the amplification reaction mix were then added onto to DNA. Amplification was performed on an Applied Biosystems 7500 thermal cycler (Grand Island, NY). Following initial denaturation at 95 °C for 10 min, amplification proceeded for 35 cycles of 95 °C for 15 s, and 45 s of annealing and extension at 60 °C. A final extension was performed at 72 °C for 10 min. Table S1 describes primers used in PCR and RT-PCR.

TaqMan real-time reverse-transcription-PCR was performed as described in the CDC protocol for real-time RTPCR detection of influenza A (H1N1) virus for 35 cycles on an Applied Biosystems 7500 thermal cycler (Grand Island, NY) (Influenza 2009). Briefly, five microliters of RNA at 10^6 copies/μL was used as the template in each reaction combined with a mastermix from Invitrogen's Superscript III Platinum One-Step quantitative kit. Twenty microliters of the amplification reaction mix were then added directly to the reaction mixture.

2.5 Detection

LAMP amplification results were analyzed by 2 % agarose gel electrophoresis and LFD strips (Ustar Biotechnologies, Hangzhou, China). LFD strips consist of a sample pad where the 10 μl sample is loaded, a conjugate pad that contains streptavidin-conjugated gold nanoparticles, a detection strip where the control and test lines are striped, and an absorbent pad to direct wicking. During amplification, loop primers tagged with FAM and biotin are incorporated into the amplicons, the biotin probe binds to the streptavidin conjugated beads, which can then aggregate at the test line (anti-fluorescein), forming a visible line to indicate a positive LAMP reaction. The control line (biotin) binds excess streptavidin beads, creating a visible positive control to show whether the flow strip worked properly.

tHDA amplicons were analyzed using 10 % acrylamide gel electrophoresis and LFD strips. tHDA amplicons contain a biotinylated primer and FAM-labeled probe that bind to the LFD strips as described above. The PCR and RT-PCR amplification results were analyzed via 10 % polyacrylamide gel electrophoresis. These did not include LFD strip analysis because biotin and FAM were not included in the primer designs.

2.6 Image analysis and quantification

LFD strips were imaged using either a Nikon D60 camera with F16 aperture at ⅓ second shutter speed or with an iPhone 5 camera on automatic setting. Because each strip contained an internal control line, both methods resulted in acceptable image quality and no post-processing was required for line intensity analysis. LFD test and control strip intensities were analyzed using the Gel Analysis feature in ImageJ (NIH, Bethesda, MA) as described previously (Linnes et al. 2014). The intensity of the control line was divided by the intensity of the test line for each LFD strip to obtain the percentage of control intensity for each sample.

2.7 Statistical analysis

To examine if materials had an effect on water absorbency, an Analysis of Variance (ANOVA) was used followed by a post hoc Tukey's Honest Significant Difference (HSD) to determine which materials differed from one another at an alpha level of 0.05. To determine if nucleic acid amplification in each experimental condition was statistically significant, LFD strip intensity for each material was compared to the experimental negative control intensity using a Dunnett's test with alpha set to 0.05.

3 Results

3.1 Materials characterization

SEM reveals the highly variable surface characteristics of the paper materials chosen in the study, as shown in Fig. 1. CHR and GF have long fibrous features that are intertwined, while PES and NC include tortuous pores, and PC has short through-hole pores due to track etching. The 0.2 μm pores in the PC membrane and the regenerated NC pores are visible only at the high (5000×) magnification (Fig. 1h and j).

Characterization of the porous nature of the materials revealed significant differences in the materials' overall porosity and number of pores, as well as the area and diameter of these pores. As seen in Table 1, the porosity measurements of the materials indicated that the PC has substantially lower porosity than the other materials with 89 % of the surface area being solid. CHR had the largest number of "pores" due to the space between individual fibrils that made up the larger fibers.

The water absorbency measurements for each paper material are shown in Fig. 2. GF absorbed the most water, an average of 88 μl/cm^2 (± 4.2 μl/cm^2). Despite their differing surface features, CHR and PES absorbed similar volumes of liquid and were not statistically significantly different from one another ($p > 0.05$), with averages of 46 and 37 μl/cm^2 (± 2.3 and 6.4 μl/cm^2, respectively). As might be expected from the minimal porosity, PC absorbed the least liquid of the sampled matrices at 14 μl/cm^2 (± 0.4 μl/cm^2). However, NC, while highly porous, did not absorb significantly more liquid than the PC ($p > 0.05$) at an average of 20 μl/cm^2 (± 5.8 μl/cm^2).

Using these water absorbency values, the size of each paper material that was required to absorb the full volume of an amplification reaction mix (25 μl) was calculated. The CHR, PES, PC, GF, and NC were cut into the corresponding size: 0.6, 0.6, 1.8, 0.3, and 0.9 cm^2, respectively, in order to perform nucleic acid amplification entirely within the paper matrices without excess reaction liquid.

3.2 LAMP

3.2.1 LAMP in the presence of membranes, with excess liquid—Isothermal amplification of both *B. pertussis* DNA and Influenza A (H1N1) RNA via LAMP and RT-LAMP, respectively, occurred in the presence of the 6 cm diameter hole-punched pieces of PES, and PC. Along with the positive control, amplification in PES and PC membranes was statistically significantly greater than the negative controls ($p < 0.005$ for each).

Amplification was inhibited by the presence of CHR, GF and NC, as determined by agarose gel electrophoresis and LFD strips, shown in Fig. 3. While statistically significant amplification for CHR was shown in the Influenza RNA assays ($p < 0.05$), this was not the case for the *B. pertussis* DNA samples. Amplification in CHR, GF, and NC was always inhibited compared to the matched positive control and, in the case of GF and NC, no amplification occurred in at least one of the three samples for both the DNA and RNA LAMP assays.

3.2.2 LAMP within membranes—LAMP and RT-LAMP resulted in successful amplification of *B. pertussis* DNA and Influenza A (H1N1) RNA, respectively, when performed completely within the PES and PC matrices. PES, PC, and the positive control all resulted in statistically significant amplification compared to the negative control for both *B. pertussis* and Influenza A (H1N1) ($p < 0.005$ and $p < 0.001$, respectively). However, the amplification was inhibited when performed within CHR, GF and NC matrices, as determined by altered band patterns in agarose gel electrophoresis and fainter test lines in the LFD strips, shown in Fig. 3. While not statistically significantly different from the negative control, some amplification did occur in experimental replicates in the presence of CHR for both *B. pertussis* DNA and Influenza A (H1N1) RNA. Additionally, faintly detectable RNA amplification occurred within the GF matrix as well, however, these were not statistically significant versus the negative control.

3.3 tHDA

3.3.1 tHDA in the presence of membranes, with excess liquid—As shown in Fig. 4, tHDA amplification in the presence of PES and PC papers, as well as the positive control, resulted in statistically significantly greater amplification than the negative control ($p < 0.05$ for each membrane amplifying *C. trachomatis* and *N. gonorrhoeae*). tHDA amplification of *C. trachomatis* and *N. gonorrhoeae* DNA was inhibited by CHR, GF, and NC membranes. While CHR material allowed for DNA amplification by tHDA in all experimental trials, the quantity of amplification product was highly variable and was not significantly different from the negative controls.

3.3.2 tHDA within membranes—tHDA within paper matrices resulted in consistent amplification of *N. gonorrhoeae* DNA using both the PES matrices and the positive, paper-free controls according to LFD strip detection ($p < 0.05$ compared to negative control). In contrast, *C. trachomatis* DNA was statistically significantly different from the negative control using only the PES matrices ($p < 0.05$). While substantial amplification occurred in each of the *C. trachomatis* positive, paper-free, controls, it was not statistically significantly different than the negative controls ($p = 0.05$) due to variability in the quantity of amplification product. CHR membranes resulted in amplification of *C. trachomatis* DNA in some, but not all, experiments and were not statistically significant compared to the negative control. Some *C. trachomatis* and *N. gonorrhoeae* DNA amplification occurred in all PC samples, but this was never greater than 50% of the control line intensity and was not statistically significant. As in tHDA samples with excess liquid, the GF and NC samples were not statistically different from the negative control samples for either *C. trachomatis* or *N. gonorrhoeae*.

3.4 PCR

PCR and RT- PCR were inhibited for all DNA and RNA samples in the presence of the 6 mm hole punch papers. Only the positive, paper-free, nucleic acid controls amplified for any of the four pathogen nucleic acids tested (*B. pertussis*, Influenza A (H1N1), *C. trachomatis, N. gonorrhoeae*). PCR was also inhibited when performed within the paper matrices with no excess liquid. No DNA amplified from *B. pertussis, C. trachomatis*, or *N. gonorrhoeae* in any sample except for the positive, paper-free, controls. However, RNA from Influenza A (H1N1) did amplify when RT-PCR was performed within PES membranes without excess liquid, but not within any of the other matrices. This unexpected result occurred in each of the three replicate experiments performed (Fig. S1).

4 Discussion

To thoroughly investigate the effect of various membrane supports on isothermal amplification, we compared the materials using four different pathogens and three amplification reaction schemes. This process was designed to account for variability in sequences, primer design, and reaction specific optimizations of component concentrations. In addition, we compared an RNA virus, Influenza A, in RT-LAMP reactions to show that these isothermal amplification results were independent of the nucleic acid template. CHR, PES, and PC all had statistically significant amplification using LAMP in the presence of membranes when excess liquid was available. The 6 mm coupons of the materials did not hold a full 25 μl reaction but allowed for additional liquid surrounding the material in which the reaction could also proceed. Therefore, additional tests were performed with larger material samples that held exactly 25 μl of liquid in order to test amplification directly within the matrix without excess liquid. PES and PC yielded statistically significant amplification using LAMP within membranes without the excess liquid. In tHDA experiments, amplification occurred in the presence of PES and PC when excess liquid was available, but only PES allowed for statistically significant amplification within membranes themselves.

The results of these two experiment setups (with and without excess liquid) were not equivalent. Thus, while some materials, such as CHR and PC, do not inhibit amplification merely by being present in the reaction mix, the amplification reactions cannot proceed efficiently when performed entirely within the membrane. This would indicate that, for these materials, amplification is only occurring in the free bulk liquid rather than within the pores of the material. In contrast, materials such as GF and NC, are often marketed for their protein and/or nucleic acid binding properties. This efficient binding likely explains the amplification inhibition when either of these two materials was present in reactions. If polymerase or DNA were bound to the surface, they would be incapable of amplification even if excess liquid were present.

PCR was completely inhibited in the presence of all membranes when excess liquid was available. However, the Influenza H1N1 RT-PCR did amplify when performed entirely within PES. The additional reverse transcriptase enzyme or components in the proprietary Superscript III enzyme mix may have had a protective effect on the RNA amplification. Previously published results by Gan et al. captured and amplified DNA on 3 mm diameter

GE brand CHR and Fusion 5 filter papers of various particle retention sizes (Gan et al. 2014). In Gan's study, PCR amplification occurred using each of the membranes, although this was inhibited compared to the control DNA without the membranes. The significantly smaller area of these membranes, 0.07 cm^2 compared to 0.28 cm^2 used in our present study's amplification in the presence of membranes may explain the minimal inhibition of the 25 μl PCR reactions in Gan et al.'s work compared to the complete inhibition of PCR seen herein. This would support our hypothesis that amplification occurs only in the bulk liquid rather than in the pores of CHR and similar materials.

Results from the present study confirm our previous observations that led us to use CHR as a support for *C. trachomatis* DNA capture with excess tHDA reagents in solution during amplification (Linnes et al. 2014). However, they differ from a previous study by Rohrman et al. that also briefly investigated inhibitory properties of various materials on a different isothermal amplification scheme, recombinase polymerase amplification (RPA) (Rohrman and Richards-Kortum 2012). These experiments indicated that bound GF was less inhibitory than CHR or GE brand Fusion 5 membranes. The bound GF was coated with polyvinylpyrrolidone (PVP) and Fusion 5 membrane is a proprietary mix of GF and polymer specifically designed to decrease absorption of macromolecules onto the surfaces. In our experiments, we tested pure GF without additional polymer binders that would alter the surface properties of the material. These showed that GF matrices alone were not suitable for either PCR or isothermal amplification. Furthermore, even the presence of the unbound GF matrix limited amplification in all cases. These findings are in agreement with previous studies of nucleic acid amplification within glass-based microfluidic chips (Taylor et al. 1997; Erill et al. 2003). These previous researchers determined that adsorption of polymerase to the high surface area of the uncoated glass chips was the main cause of PCR inhibition. This is likely the case with the GF in our present study as it contained numerous pores that led to high water absorbency.

As our native GF results were discordant with the hydrophilic PVP coated bound GF results, we sought additional information from the manufacturers of all of the membranes used in our study regarding membrane processing and surface treatments. We learned that the PC utilized in our study was coated with PVP to increase its hydrophilicity. Although the PVP could be leached from the membranes when washed extensively, we did not use any pre-washing step and therefore must assume the PVP was in the reaction, initially coating the PC though it may have been eluted from the PC into the solution during the amplification process. PES membranes also were surface treated by the manufacturer to enhance their hydrophilicity in a proprietary process, such as a weak zwitterionic surface treatment. Other membranes were confirmed to be free of surface and bulk treatments that might change the base membrane properties. The hydrophilic coatings may explain the somewhat protective effect of the PC and PES membranes compared to the other materials and serve as a key starting point for choosing efficient amplification supports in the future.

In many ways, tHDA and LAMP isothermal amplification reactions are similar to their predecessor PCR. However, our findings indicate that the amplification, or lack thereof, using PCR gives no indication of a material's suitability for isothermal amplification methods. In fact, PCR was inhibited by all of the materials tested, while LAMP and tHDA

showed statistically significant amplification both within PES and in the presence of CHR and PC. Both tHDA and LAMP utilize the same overall principles of polymerase-based amplification as PCR. However, these isothermal amplification schemes require more complicated reaction mixtures including helicase and single stranded binding proteins for tHDA and 2–4 additional primer pairs for LAMP. Previous studies have shown LAMP to be more robust than PCR to inhibitors such as serum, urine, and non-target DNA, though no such studies of tHDA compared to PCR have been performed to date (Enosawa et al. 2003; Poon et al. 2006; Kaneko et al. 2007). The researchers testing LAMP hypothesized that the LAMP robustness may be related to the differences in polymerases used for PCR reactions compared to isothermal reactions. The exonuclease, Taq polymerase, is traditionally used for PCR while LAMP and HDA both utilize strand displacing, Bst polymerase. The addition of high concentrations of molecular crowding components used to enhance amplification efficiency in isothermal reactions, such as ficoll 400 in tHDA and betaine in LAMP, may further stabilize these reactions against potential interactions with the surfaces of the paper materials.

Measured pore diameters were in good agreement with the manufactures values for PC and NC as these surfaces had fairly regular feature sizes (see Fig. 1). The average pore diameter of PES was significantly higher than the nominal pore size according to the manufacturer (0.2 μm). However, the nominal pore size is a measure of the smallest particle that can pass through the material, which is not measurable by image analysis of the surface. The porosity of the dried materials may also underestimate that of the hydrated states of the materials. This is particularly significant for CHR, which had visible swelling in response to the addition of fluids.

These swelling characteristics may lead to uneven wetting of membranes and may have also contributed to the high variability in the color intensity of the control lines of the LFD strip membranes as well (Figs. 2b and 3b.). This phenomena has been described previously by Wong and Tse who discussed the effects of wicking and porosity in NC and Fusion 5 membranes (Wong and Tse 2009). We had initially considered setting the intensity of the test line of the LFD as the only independent variable when analyzing the amplification efficiency, as performed in studies by Rohrman et al. and by Warren et al. when designing in-house made LFD strips (Rohrman et al. 2012; Warren et al. 2014). However, this would not have taken into account the validity of the LFD strips' internal control results. We also considered additional post-processing of images to artificially normalize to the background intensity of the LFD strips. However, this would have skewed results of strips that had higher background coloring. Our purpose was not to investigate previously validated commercially developed test strips, but simply to use them to visualize the amplification products of our assays. Therefore, we took advantage of the available control lines to normalize our results. Finally, we imaged our LFD strips after they had completely dried in order to ensure complete washing of the strips for comparable imaging of each set of experiments. We have observed that the intensity of the test and control lines increased slightly once the samples are dried. Drying of the LFD strip could potentially have allowed for the test strips to increase the intensity of results further. However, in preliminary tests, we did not see any difference in relative intensity of the control and test lines compared to those imaged after the drying process. Using the test line intensity as a percentage of the

control lines accounted for the intensity changes upon drying as well as the relative background intensities in the LFD strips.

A previous study comparing the effects of pore sizes among NC membranes, showed that pore size was inversely related to protein binding (Low et al. 2013). Low et al. found that an average pore size of 11 μm NC bound significantly more bovine serum albumin than equivalent NC membranes with average pore sizes of 15 μm and 29 μm. This effect is likely related to the higher surface area available to bind in these small pore size membranes. However, in our present study, pore size itself was not correlated to amplification efficiency. PES had similar average pore size as NC (0.51 μm and 0.45 μm, respectively) and PC membranes had even smaller, 0.23 μm diameter pores. Yet, unlike the NC, which completely inhibited amplification, these two membranes had the most successful LAMP and tHDA reactions of all the membranes studied. A more likely explanation is the hydrophilic nature of the PC and PES used. According to the manufacturer, the NC used in our study is known to bind approximately 80 μg/cm^2 of protein and up to 150 μg/cm^2 of single stranded DNA such as primers (Whatman 2004; Buckingham and Flaws 2007). In contrast the PES membranes used in our study binds only 15 μg/cm^2 of goat anti-rabbit IgG from a 1mg/ml solution (Millipore 2002). The much lower binding of the assay components to the membrane likely allows the reaction to proceed in the amplification solution trapped within the membrane pores.

One of the many advantages of paper-fluidic diagnostics is their low cost. We have included costs of the materials at the time of writing the manuscript, in Table 2 for comparison (cost of large-scale manufacturing was not determined). While PES is viewed by some as an expensive material, we found that in our laboratory scale, it was significantly less expensive than commonly used LFD membrane, NC (8.4 cents/cm^2 for PES compared to 32 cents/cm^2 for NC). GF and PC were marginally cheaper at 5.5 cents/cm^2 and 3.1 cents/cm^2, respectively. None of these compares favorably to the ultra-low-cost of CHR, 0.18 USD/cm^2. Of note, all but PC can be purchased in rolls, which would significantly reduce their cost/cm^2 in scaled up manufacturing. Ultimately, the small amount of membrane used, contributes proportionally little to the total cost of these molecular devices. The isothermal enzyme mixes are a far greater portion of the cost of these molecular tests at this prototype scale. The price of paper-based molecular diagnostics is significantly greater than lateral flow assays alone. However, the advantage of highly sensitive and specific detection from a wide array of nucleic acid targets will likely outweigh these cost constraints in the future. The optimal design of amplification membranes is essential to enable these gold-standard molecular diagnostic tests to be performed at the point of care.

5 Conclusions

Our findings provide insight into the efficacy of isothermal amplification in various materials choices under consideration for paper-based molecular diagnostic devices, and results suggest that the use of PES membranes enables the widest range of successful amplification reactions among the tested materials. To systematically investigate these effects, we utilized two different isothermal reactions schemes covering four distinct nucleic acid targets and compared three current diagnostic membranes (CHR, GF, and NC) as well

as two additional porous materials (PES, PC) to paper-free positive and negative amplification controls.

The effects of these materials on isothermal reactions could not be predicted by PCR amplification in the materials, nor classified by their pore sizes or microstructures. The mere presence of GF and NC membranes strongly inhibited LAMP and tHDA reactions. The strong protein and DNA binding properties of GF and NC membranes likely prevents these biomolecules from participating in amplification reactions. While reduced, LAMP and tHDA still occurred in the presence of CHR. However, when the size of the CHR membrane was increased to absorb the entire liquid reaction volume, amplification was further inhibited. While the presence of PC itself did not inhibit either LAMP or tHDA amplification, tHDA reactions were impeded when performed entirely within the pores of the membrane. Only PES allowed for efficient LAMP and tHDA in all reaction conditions, even though it has not been widely used in rapid diagnostic tests to date. These results suggest that materials selection should focus on hydrophilic membranes, such as surface treated PES, for rapid molecular diagnostics in point-of-care applications.

Supplementary Material

Refer to Web version on PubMed Central for supplementary material.

Acknowledgments

This work was funded by NIH/NIAID F32-AI110023 (JCL) and NIH U54-EB015403 (CMK, NMR, LL) as well as the National Science Foundation Graduate Research Fellowship (NMR) and a Diversity Administrative Supplement under NIH U54-EB015403-S1 (CMK, NMR).

References

Ali MM, Aguirre SD, Xu YQ, Filipe CDM, Pelton R, Li YF. Detection of DNA using bioactive paper strips. Chem. Commun. 2009; 43:6640–6642.

Buckingham, L.; Flaws, ML. Molecular Diagnostics: Fundamentals, Methods, & Clinical Applications. Philadelphia: F.A. Davis; 2007.

Connelly JT, Rolland JP, Whitesides GM. “Paper machine” for molecular diagnostics. Anal. Chem. 2015; 87(15):7595–7601. [PubMed: 26104869]

Cordray MS, Richards-Kortum RR. A paper and plastic device for the combined isothermal amplification and lateral flow detection of *Plasmodium* DNA. Malar. J. 2015; 14(1):472. [PubMed: 26611141]

Enosawa M, Kageyama S, Sawai K, Watanabe K, Notomi T, Onoe S, Mori Y, Yokomizo Y. Use of loop-mediated isothermal amplification of the IS900 sequence for rapid detection of cultured *Mycobacterium avium* subsp. paratuberculosis. J. Clin. Microbiol. 2003; 41(9):4359–4365. [PubMed: 12958269]

Erill I, Campoy S, Erill N, Barbe J, Aguilo J. Biochemical analysis and optimization of inhibition and adsorption phenomena in glass-silicon PCR-chips. Sensors Actuators B Chem. 2003; 96(3):685–692.

Ferreira, T.; Rasband, WS. ImageJ User Guide — IJ 1.46. U.S. National Institutes of Health; 2010–2012. imagej.nih.gov/ij/docs/guide/

Gan WP, Zhuang B, Zhang PF, Han JP, Li CX, Liu P. A filter paper-based microdevice for low-cost, rapid, and automated DNA extraction and amplification from diverse sample types. Lab Chip. 2014; 14(19):3719–3728. [PubMed: 25070548]

World Health Organization. CDC Protocol of Realtime RTPCR for Influenza A(H1N1). Geneva: World Health Organization; 2009.

Kamachi K, Toyoizumi-Ajisaka H, Toda K, Soeung SC, Sarath S, Nareth Y, Horiuchi Y, Kojima K, Takahashi M, Arakawa Y. Development and evaluation of a loop-mediated isothermal amplification method for rapid diagnosis of *Bordetella pertussis* infection. J. Clin. Microbiol. 2006; 44(5):1899–1902. [PubMed: 16672435]

Kaneko H, Kawana T, Fukushima E, Suzutani T. Tolerance of loop-mediated isothermal amplification to a culture medium and biological substances. J. Biochem. Biophys. Methods. 2007; 70(3):499–501. [PubMed: 17011631]

Kubo T, Agoh M, Mai le Q, Fukushima K, Nishimura H, Yamaguchi A, Hirano M, Yoshikawa A, Hasebe F, Kohno S, Morita K. Development of a reverse transcription-loop-mediated isothermal amplification assay for detection of pandemic (H1N1) 2009 virus as a novel molecular method for diagnosis of pandemic influenza in resource-limited settings. J. Clin. Microbiol. 2010; 48(3):728–735. [PubMed: 20071551]

Li CC, Beck IA, Seidel KD, Frenkel LA. Persistence of human immunodeficiency virus type 1 subtype B DNA in dried-blood samples on FTA filter paper. J. Clin. Microbiol. 2004; 42(8):3847–3849. [PubMed: 15297546]

Li J, Macdonald J. Advances in isothermal amplification: novel strategies inspired by biological processes. Biosens. Bioelectron. 2015; 64:196–211. [PubMed: 25218104]

Linnes JC, Fan A, Rodriguez NM, Lemieux B, Kong H, Klapperich CM. Paper-based molecular diagnostic for *Chlamydia trachomatis*. RSC Adv. 2014; 4(80):42245–42251. [PubMed: 25309740]

Liu C, Geva E, Mauk M, Qiu X, Abrams WR, Malamud D, Curtis K, Owen SM, Bau HH. An isothermal amplification reactor with an integrated isolation membrane for point-of-care detection of infectious diseases. Analyst. 2011; 136(10):2069–2076. [PubMed: 21455542]

Low SC, Shaimi R, Thandaithabany Y, Lim JK, Ahmad AL, Ismail A. Electrophoretic interactions between nitrocellulose membranes and proteins: Biointerface analysis and protein adhesion properties. Colloids Surf. B: Biointerfaces. 2013; 110:248–253. [PubMed: 23732801]

Millipore. 33 mm Medical Millex Filter Units with Millipore Express membrane. Vol. 2. Bedford, MA: Millipore Corporation; 2002. Rev. A 7/02 02-208

Poon LLM, Wong BWY, Ma EHT, Chan KH, Chow LMC, Abeyewickreme W, Tangpukdee N, Yuen KY, Guan Y, Looareesuwan S, Peiris JSM. Sensitive and inexpensive molecular test for falciparum malaria: Detecting *Plasmodium falciparum* DNA directly from heat-treated blood by loop-mediated isothermal amplification. Clin. Chem. 2006; 52(2):303–306. [PubMed: 16339303]

Reischl U, Lehn N, Sanden GN, Loeffelholz MJ. Real-time PCR assay targeting IS481 of Bordetella pertussis and molecular basis for detecting *Bordetella holmesii*. J. Clin. Microbiol. 2001; 39(5): 1963–1966. [PubMed: 11326023]

Rodriguez NM, Linnes JC, Fan A, Ellenson CK, Pollock NR, Klapperich CM. Paper-based RNA extraction, *in situ* isothermal amplification, and lateral flow detection for low-cost, rapid diagnosis of influenza A (H1N1) from clinical specimens. Anal. Chem. 2015; 87(15):7872–7879. [PubMed: 26125635]

Rodriguez NM, Wong WS, Liu L, Dewar R, Klapperich CM. A fully integrated paperfluidic molecular diagnostic chip for the extraction, amplification, and detection of nucleic acids from clinical samples. Lab Chip. 2016; 16(4):753–763. [PubMed: 26785636]

Rohrman BA, Leautaud V, Molyneux E, Richards-Kortum RR. A lateral flow assay for quantitative detection of amplified HIV-1 RNA. PLoS One. 2012; 7(9):e45611. [PubMed: 23029134]

Rohrman BA, Richards-Kortum RR. A paper and plastic device for performing recombinase polymerase amplification of HIV DNA. Lab Chip. 2012; 12(17):3082–3088. [PubMed: 22733333]

Taylor TB, WinnDeen ES, Picozza E, Woudenberg TM, Albin M. Optimization of the performance of the polymerase chain reaction in silicon-based microstructures. Nucleic Acids Res. 1997; 25(15): 3164–3168. [PubMed: 9224619]

Warren AD, Kwong GA, Wood DK, Lin KY, Bhatia SN. Point-of-care diagnostics for noncommunicable diseases using synthetic urinary biomarkers and paper microfluidics. Proc. Natl. Acad. Sci. U. S. A. 2014; 111(10):3671–3676. [PubMed: 24567404]

Whatman. Protran® Nitrocellulose Membranes. Proteomics and Glycomics Brochure. Florham Park: Whatman, Inc; 2004. p. 6

Wong, RC.; Tse, HY. Lateral Flow Immunoassay. New York: Springer; 2009.

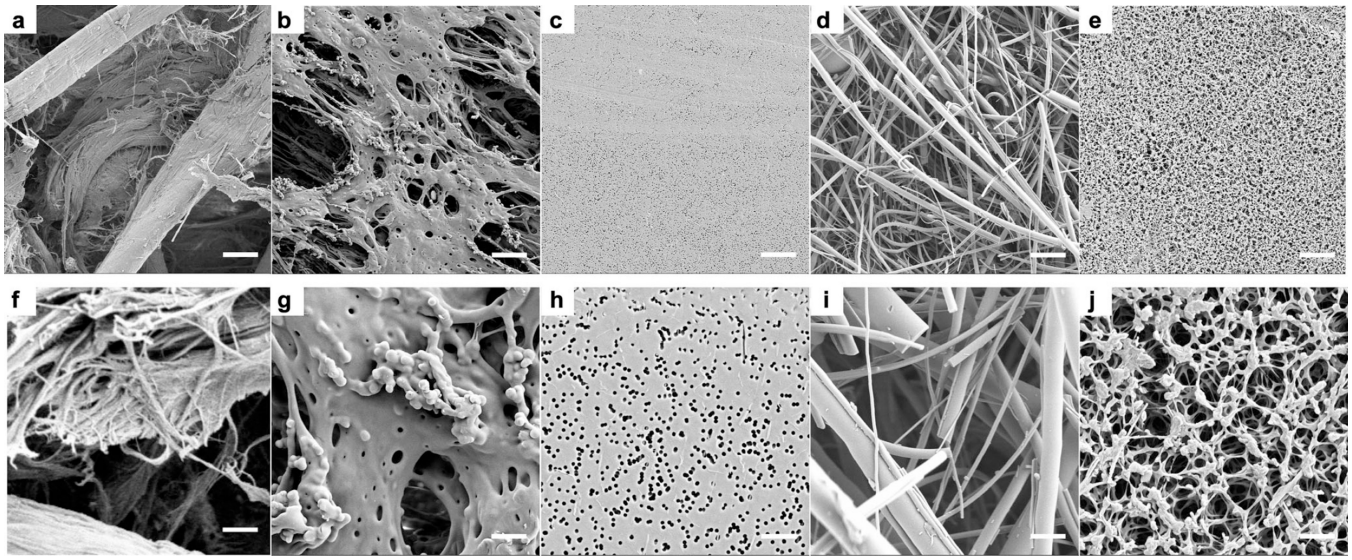

Fig. 1.

Scanning electron micrograph of CHR (**a, f**), PES (**b, g**), PC (**c, h**), GF (**d, i**), and NC (**e, j**) at 1000× (**a–e**) and 5000× (**f–j**) magnification. *Scale bars* represent 10 μm (**a–e**) and 2 μm (**f–j**)

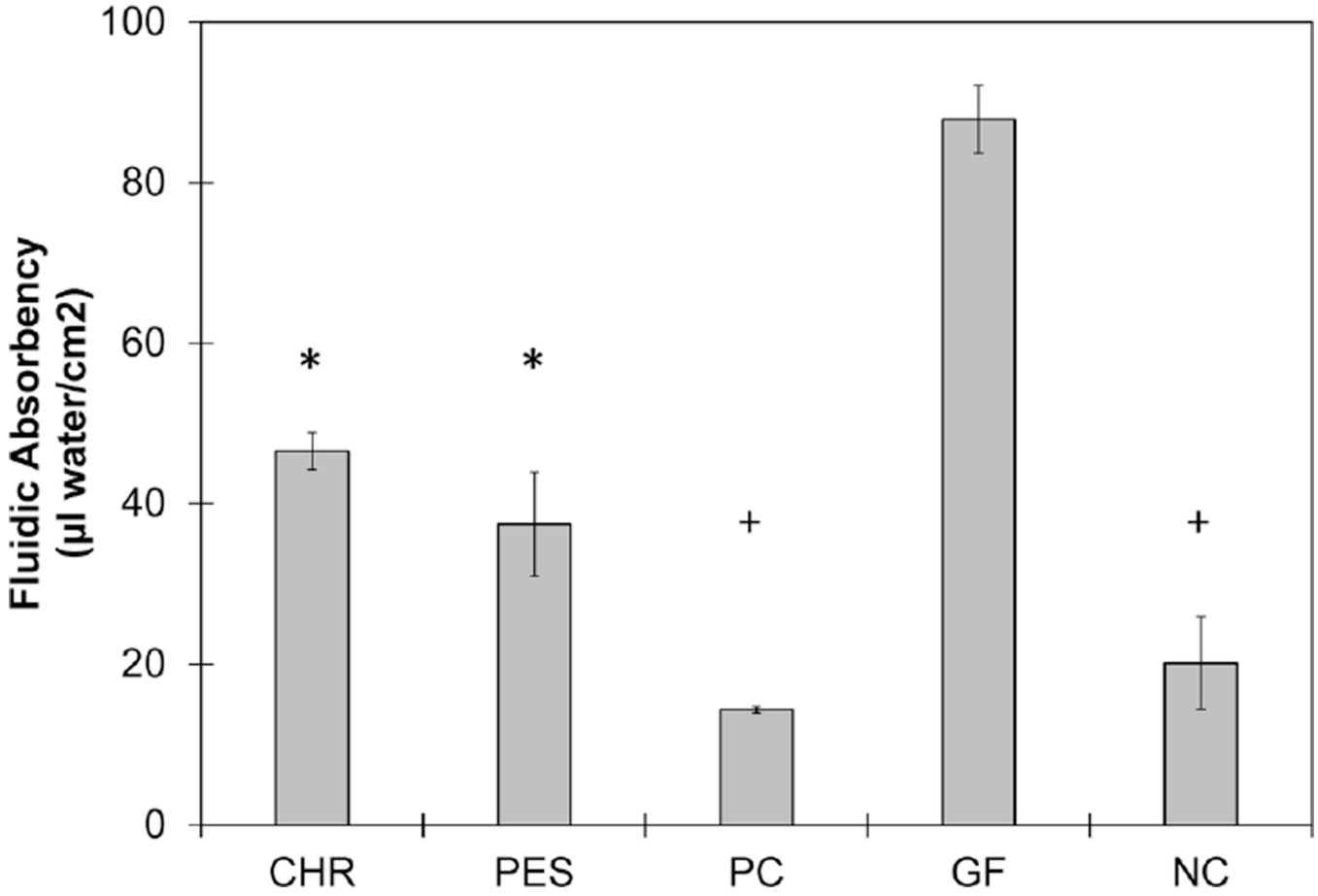

Fig. 2.

Fluidic absorbency of 1 cm^2 materials. Average absorbency +/− standard deviations are shown (n = 5 for each sample type). Materials with similar symbols (* or +) are not statistically significantly different than one another using a one-way ANOVA followed by Tukey's HSD test

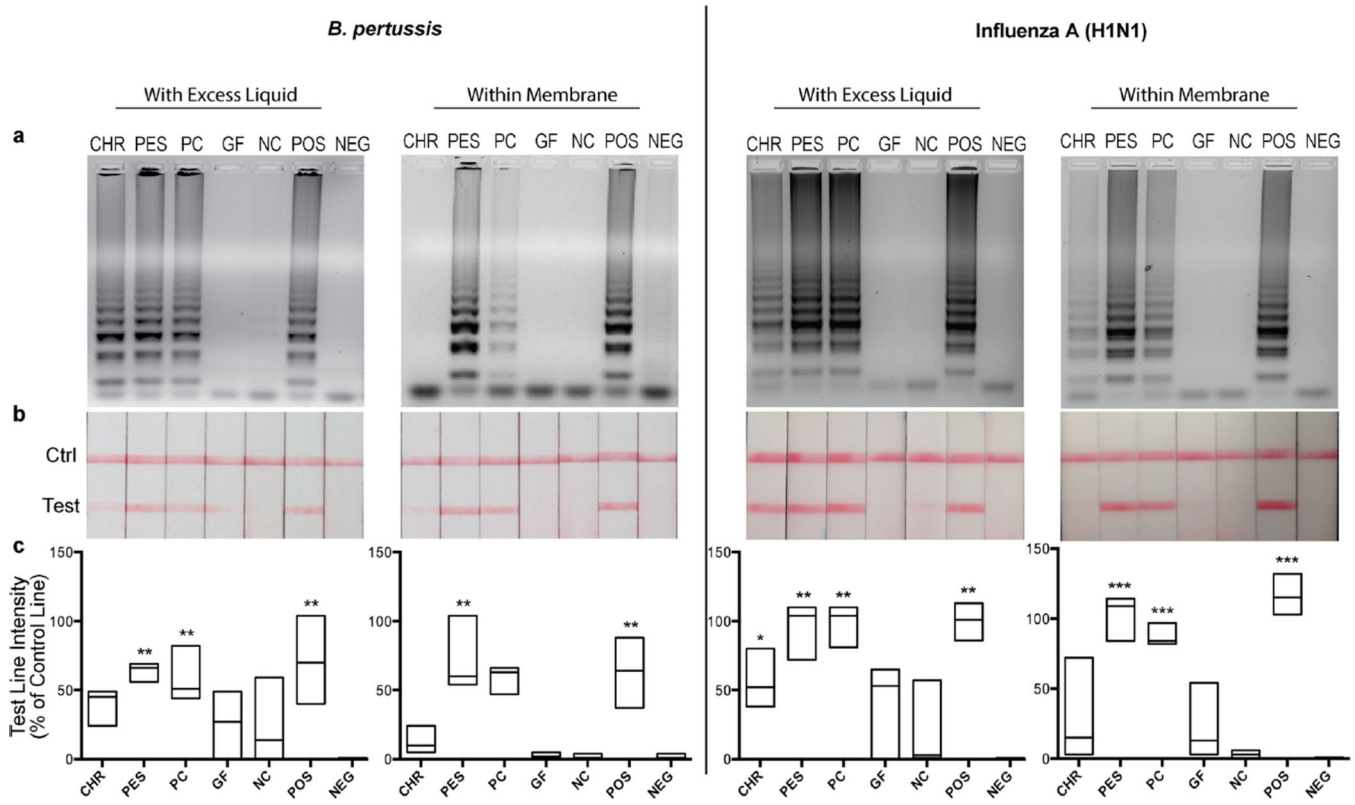

Fig. 3.

Results of LAMP performed on *B. pertussis* (*Left*) and Influenza A (H1N1) (*Right*). Detection by agarose gel electrophoresis (**a**) and LFD strips (**b**). Intensity of the LFD test line as a percentage of the control line in the strips is shown in (**c**). Box plots indicate the minimum, maximum, and median intensities for each sample. (*$p < 0.05$, **$p < 0.005$, ***$p < 0.001$ using Dunnett's test versus the negative control)

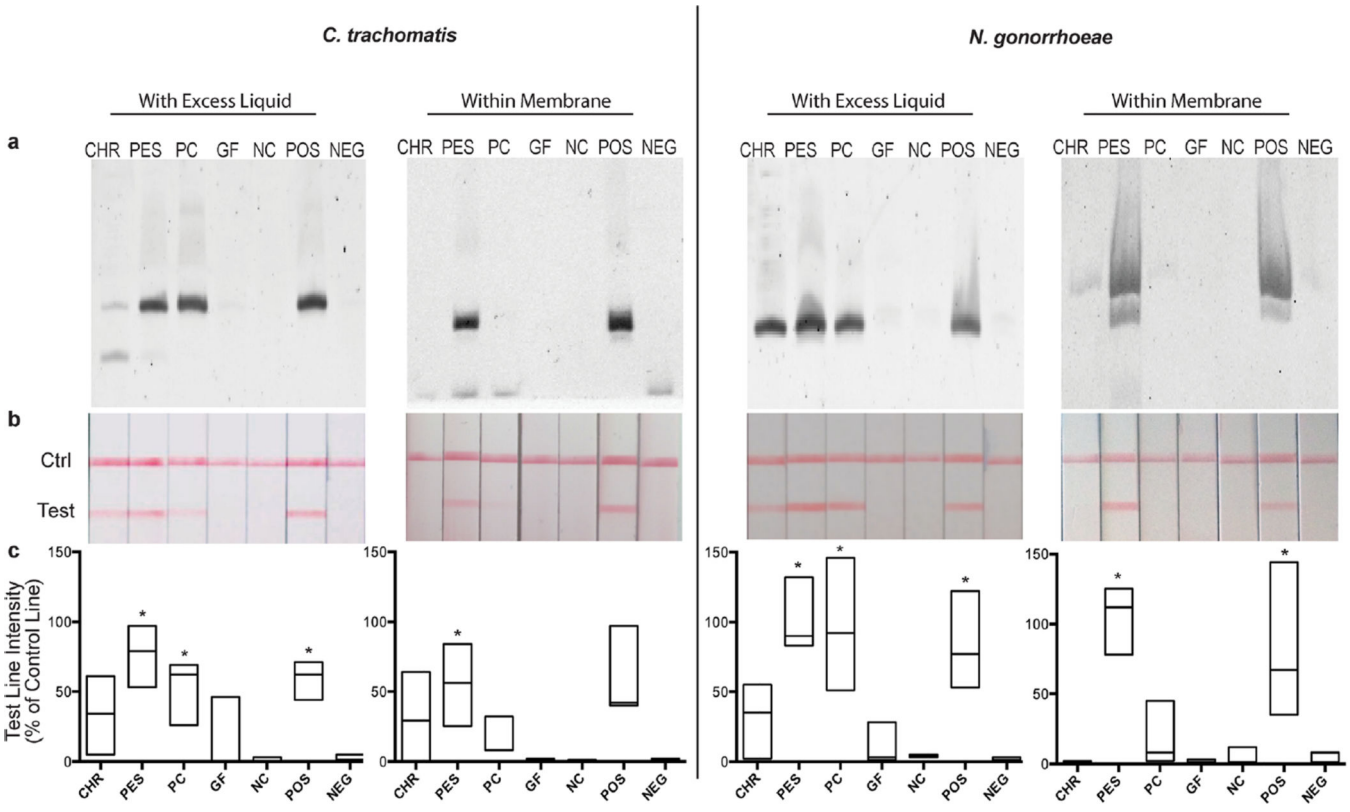

Fig. 4.

Results of tHDA performed on *C. trachomatis* (*Left*) and *N. gonorrhoeae* (*Right*). Detection by agarose gel electrophoresis (**a**) and LFD strips (**b**). Intensity of the test line as a percentage of the control line in the strips is shown in (**c**). Box plots indicate the minimum, maximum, and median intensities for each sample. (*$p < 0.05$ using Dunnett's test versus the negative control)

Table 1

Porosity of materials. Average (± standard deviation) reported for the pore area and diameter of pores analyzed

	Porosity (%)	Pores per 100 um^2	Pore area (um^2)	Pore diameter (um^2)
CHR	39	—	—	—
PES	45	215	0.21 ± 2.16	0.51 ± 1.66
PC	11	266	0.04 ± 0.03	0.23 ± .20
GF	53	—	—	—
NC	41	259	0.16 ± .35	0.45 ± 0.66

Table 2

Comparison of materials examined and results of the present study

Material	Current uses	Fluidic absorbency (μl/cm^2)	Porosity (%)	Isothermal Amplification[a]	Cost[b] (USD/cm^2)
Cellulose (CHR)	• LFD sample pad • Chromatography	46	39	+/−	0.0018
Polyethersulfone (PES)	• Cell capture • Filtration	37	45	++	0.84
Track Etched Polycarbonate (PC)	• Cell capture • Filtration	14	11	+	0.31
Unbound Glass Fiber (GF)	• LFD conjugate pad • Filtration • Nucleic acid binding	88	53	−	0.55
Nitrocellulose (NC)	• LFD membrane • Protein and nucleic acid binding	20	41	−	0.32

[a]Isothermal efficacy as determined by statistically significant amplification in the current publication (++ indicates amplification in all cases, + indicates amplification in most cases, +/− indicates amplification some of the time, − indicates no significant amplification)

[b]Cost in U.S. dollars (USD) per cm^2 at the time of writing